OPEN GEOMECHANICS

Review History for "Response of granular material under combined principal stress value and orientation change in 3D space"

Eleni Gerolymatou *2022*

Summary

The paper was sent to two Reviewers: Dr. Konstantinos Karapiperis, ETH Zurich (Reviewer 1) and Dr. Lukas Knittel, Karlsruhe Institute of Technology (Reviewer 2). The two reviewers remained anonymous during the entire revision process. After the reviewing process was completed, the reviewers decided to disclose their identity.

In the first round of review, both reviewers and the Editor recommended that minor revisions be made to the manuscript before it could be published.

After minor revisions, Reviewers 1 and 2 recommended accepting the manuscript without any required modifications. The Editor decided to accept the manuscript without further modification.

Remarks concerning typos have been omitted for the sake of brevity.

Review Round 1

Reviewer 1 (Konstantinos Karapiperis)

The authors investigate the effect of principal stress value and orientation change on the response of spherical assemblies on fixed-plane as well as more general 3D stress paths through discrete element simulations. Appropriate micromechanical and macroscopic variables are analyzed to gain insight into the response. The methods are well described, and the authors have taken good care to present the results. I recommend that a few minor points be addressed before the manuscript is accepted for publication:

- The authors use gravitational deposition to achieve an anisotropic initial state, on which all subsequent results are based. The authors should provide a quantification of this anisotropy, e.g. through the initial fabric tensor.
- In the conclusion section, the authors claim that the fabric anisotropy variable A has a negative correlation with dilatancy D or at least that D becomes greater at smaller A value. Although the fixed-plane simulations in Fig. 9 strongly support this conclusion, the results from the more general paths in Fig. 13 hardly support it, at least visually (perhaps a quantification of this correlation can prove useful here). Can the authors provide any insight into why this is the case? One naturally wonders whether this statement has any truth in arbitrary stress paths.

- Are all DEM simulations in the study quasistatic? If yes, then the use of the phrase 'seismic load simulation' might be misleading. The authors should refer to this part of the study as 'birectional cyclic shear'.

Reviewer 2 (Lukas Knittel)

The paper presents a numerical study using the Discrete Element Method (DEM) on the response of granular material under combined principal stresses and different orientation changes in the 3D space. Cyclic and seismic loads on samples with consistent void ratios 0.686≤ e ≤ 0.689 in four measure zones are tested. Spherical particles with D_{50} = 0.225 mm, D_{min} = 0.115 mm and D_{max} = 0.305 mm were used for these observations. Plots of the accumulation of volumetric strain ε_v, equivalent shear strain γ, shear modulus G, non-coaxial angle Ψ and the dilatancy D are given. The force line boundary condition of Xue et al. L. Xue and Zhang [2019] was adopted to allow the application of principal stress in arbitrary directions. As a main result of this study with four cyclic loading types, the greatest deformations were observed under a circular stress path where the orientation of stress changes, while the principal values remain constant. For the 3D stress paths and bidirectional seismic loads the dilatancy D becomes greater at smaller fabric anisotropy A value. This results in asymmetrical development of D for stress paths that incorporate stress orientation change, causing the rapid accumulation of volumetric strain ε_v within the first few load cycles. From an experimental view, the orders of magnitude of the numerical test results might be hard to comprehend and need some more explanations in the article. Overall, the paper is well written and represents an original contribution to the field of DEM and multidimensional loading. The described DEM technique has significant potential to be more frequently applied by researchers in future. Consequently, I recommend the paper for publication with some revisions addressed below.

- Page 2: For the readers it would be helpful to add a notation overview (e.g. equivalent shear strain, dilatancy D, fabric anisotropy value A, ...).
- Page 2, right column, fourth paragraph: I recommend to explain Δl in more detail.
- Page 3, right column, fourth paragraph: why are definitions of an "Average" only in the equations (4),(5) and (6) used, but not in the other equations from (1)-(9)?
- Figure 1: Please include the range of the void ratio as well as the number of particles in the caption.
- Figure 2:
  - Page 3, the definition of mean effective stress p and deviatoric stress q is given in Eq. (2) and (3). Table 1 uses these definitions for q_{min} and q_max. The left column of Fig. 2 is similar to Towhata and Ishihara [1], but using p and q as well as a definition of the Amplitude q_ampl the reader could follow more easily.
  - What are the units of x, y and z in the right column (cf. Fig. 10 in (kPa))?
- Page 5, left column: Please refer the Figures 2b-d in the text.
- Page 5, left column, first paragraph of 3.2: Eventually, the accumulation of volumetric strain slows down to reach an asymptotic state, as discussed by Wang et al. [2019b] and Xue et al. [2019]. Eventually? This aspect should not be questioned by the authors.
- Figure 3:
  - The figures 3(a) and 3(b) should be scaled identically.
  - It's interesting to see that the test results in Fig. 3(a) for L-0-30-F with q_{max} = 30 kPa → ε_v(N = 30) ≈ $1 \cdot 10^{-4}$ are comparable to the results of Wichtmann and Knittel Wichtmann and Knittel [2019] in Fig. 17.
  - In Fig. 3(a) for S-30-30-R with $q_{max} = q_{min}$ = 30 kPa → ε_v(N = 30) ≈ $2.1 \cdot 10^{-3}$ is received. The comparison with L-0-30-F results in a factor of 20 in volumetric strain. On the physical side, this seems to be impossible. Could the authors explain these distinguish results?
  - From Fig. 3(b) for L-0-50-F → ε_v(N = 30) ≈ $1 \cdot 10^{-3}$ and S-50-50-F → ε_v(N = 30) ≈ $8.5 \cdot 10^{-3}$ a factor of 8.5 in volumetric strain can be estimated. Why does a higher amplitude take more than two times lower in volumetric strain by comparison of 3(a) and 3(b)?
  - Comparison of HS-50-50-R and S-50-50-R: could the authors describe this discrepancy even though the planes are just rotated?
- Page 5, right column, first paragraph: These results agree qualitatively with the undrained cyclic torsional tests by Towhata and Ishihara Towhata and Ishihara [1985], which showed that the liquefaction resistance of sand under a half-"8"-shaped stress path is between circular stress path and straight-line stress path. This statement is correct, however, it would be easier for the reader to depict an figure in the text with this statement.

- Figure 4:
  - The figures 4(a) and 4(b) should be scaled identically.
  - Analogous to Fig. 3 the results of the equivalent shear strain are not consistent. Could the authors explain the comparison of the test results from S-30-30-R $\bar{\gamma}(N = 30) \approx 0.3$ and S-50-50-R $\bar{\gamma}(N = 30) \approx 1.3$ as an example?

- Figure 5:
  - The presented progresses of the shear modulus G seems to be really small. Could the authors explain this physically in the text?
  - What is the cause of the spikes in G for L-0-30-F (numerical problems)?
  - S-30-30-R should be more critical as L-0-30-F, but no spikes occurred. The question is why?

- Figure 6: Please explain the differences in the amplitudes of B-0-30-R and S-30-30-R.

- Figure 9:
  - This figure shows the dilatancy D and fabric anisotropy variable A, also at the 20th cycle with greater fluctuations. Fig. 3-7 is plotted for $0 \leq N \leq 30$ but Fig. 8 for $0 \leq N \leq 10$. Did the authors receive impossible values of D for $10 \leq N \leq 30$ in Fig. 8, which could be seen in Fig. 9?

- Figure 10: Please plot N = 30 cycles in Figure 10(b).

- What is the practical relevance for N = 30 number of seismic load cycles? What is the physical time for seismic loads (of course no time dependence were considered)?

- Page 13, last paragraph of the conclusion: ... all possible influence factors, which warrants more in-depth investigations. Which ones? Please give some hints.

Review Round 1: Author Response

We would like to sincerely thank the editor's and reviewers' detailed comments on the manuscript. We have revised the manuscript based on the comments and suggestions of the reviewers, which have improved the quality of the manuscript. In the following, we have responded to the reviewers' comments on a point-by-point basis, most of which have also been reflected in the revised manuscript. For each comment, the comment is first given, followed by our response. The changes made to the manuscript are also provided in italic style and blue color after our response, if any. We hope that our response and revision will adequately address the reviewers' concerns.

Reply to Reviewer 1

We are very grateful to the reviewer for the positive comments on the study and appreciate the suggestions of the reviewer. Based on the comments, we have made revisions in the manuscript and responded to each comment below.

- The authors use gravitational deposition to achieve an anisotropic initial state, on which all subsequent results are based. The authors should provide a quantification of this anisotropy, e.g. through the initial fabric tensor.

  As suggested by the reviewer, the initial fabric tensor is calculated and shown in the article to provide a quantification of the anisotropy of the sample.

  In Page 4, left column:
  The initial anisotropic state of the sample is also measured through Eq. (9):

$$F_0 = \begin{bmatrix} 0.00943 & 0.00118 & 0.00248 \\ 0.00118 & 0.00653 & 0.00083 \\ 0.00248 & 0.00083 & 0.01587 \end{bmatrix} \tag{10}$$

  where F_{zz} =0.01587, obviously larger than F_{xx} and F_{yy}, implying that the dominant direction of contact is close to z direction (gravity direction).

- In the conclusion section, the authors claim that the fabric anisotropy variable A has a negative correlation with dilatancy D or at least that D becomes greater at smaller A value. Although the fixed-plane simulations in Fig. 9 strongly support this conclusion, the results from the more general paths in Fig. 13 hardly support it, at least visually (perhaps a quantification of this correlation can prove useful here). Can the authors provide any insight into why this is the case? One naturally wonders whether this statement has any truth in arbitrary stress paths.

We agree that clarification is needed here. The relationship between dilatancy D and the fabric anisotropy variable A is not a causal relationship, meaning that although A affects dilatancy, it does not determine it. Therefore, the apparent relationship between A and D is more complex than a simple negative correlation. In general, the observation is that under the same loading conditions, D tends to be greater for negative A, and vice versa, and a greater change in A could lead to more significant changes in D. We have changed some expressions in the article and add the linear fit equation between dilatancy D and the initial fabric anisotropy variable A for the first load cycle for all simulations, to provide a quantitative assessment, as suggested by the reviewer. It is shown that the slope of the D-A fit is negative for all of the cases, except for L-0-50-F, where A remained almost constant.

In Page 9:
Fig. 9 shows the scatter plot of dilatancy against A at the 1st, 10th and 20th cycle for the three different types of stress paths, along with the linear fit of the first cycle. It shows that there is generally more contraction tendency when A has a greater negative value. The linear fit between D and A is also plotted in Fig. 9, with the slope of the D-A fit being negative for all the cases, except for L-0-50-F, where A remained almost constant. These findings are in agreement with existing studies on stress paths with only principal stress value change [Wang et al., 2019a]. It is worth pointing out that the variation range of A under straight-line stress path is much smaller than that in the other two cases and oscillates at approximately zero even at the very beginning, resulting in near symmetrical dilatancy with respect to zero, and sign of the slope of the linear fit is not very meaningful. When principal stress orientation change is included, the variation range of A is expanded, D tends to be greater for negative A under the circular and "8"-shaped stress paths, indicating more contraction. This asymmetrical dilatancy development due to anisotropy significantly affects volumetric strain accumulation. Although the dilatancies under the circular and "8"-shaped stress paths are similar quantitatively, the accumulated volumetric strain is greater under the circular stress path due to the smaller shear modulus and greater shear strain. For HS-50-50-R, the variation range of A is also limited compared to S-50-50-R, resulting in smaller initial volumetric contraction. This shows that fabric anisotropy plays a significant role in the dilatancy and volumetric deformation of granular material, especially when stress orientation change occurs along with value change.

In Page 12, 13 and 14: *Fig. 13 shows the scatter plot of dilatancy against A at the 1st, 10th cycle for the 3D tests and also the linear fit between D and A for the first cycle. For all four stress paths, D is negatively affected by A during the first load cycle. The variation range of A is limited for D-F stress path, similar to the case of fixed stress orientation in Fig. 9, and the sample experiences mostly oscillating dilatancy and volumetric strain. As for the other three stress paths, smaller value of A is achieved as the orientation of stress changes, resulting in enhanced contraction and subsequent accumulation of positive volumetric strain, similar to the situation when principal stress is within a fixed plane.*

In Page 13, conclusions section:
Paragraph 2:
Under the same loading conditions, D tends to be greater for negative A, and vice versa, indicating that fabric anisotropy plays a major role in the dilatancy, and subsequently volumetric deformation, of granular material under the combined effect of principal stress value and orientation change.
Paragraph 3:
The relationship between D and A becomes more complex, but still generally shows that D tends to be negatively affected by A.

- Are all DEM simulations in the study quasistatic? If yes, then the use of the phrase 'seismic load simulation' might be misleading. The authors should refer to this part of the study as 'birectional cyclic shear'.

Owing to the stress control mode used in the article, all the simulations conducted here are quasistatic and it is mentioned clearly in the article this time. Considering the reviewer's suggestion, we have changed the 'seismic load simulation' to 'seismic stress path simulation' in Page 9-12.

In Page 3: *All tests are simulated under quasistatic conditions.* In Page 10: *Also, quasistatic simulations are conducted here instead of the real time dependent dynamic process of earthquakes to focus on the combined effect of principal stress value and direction change.*

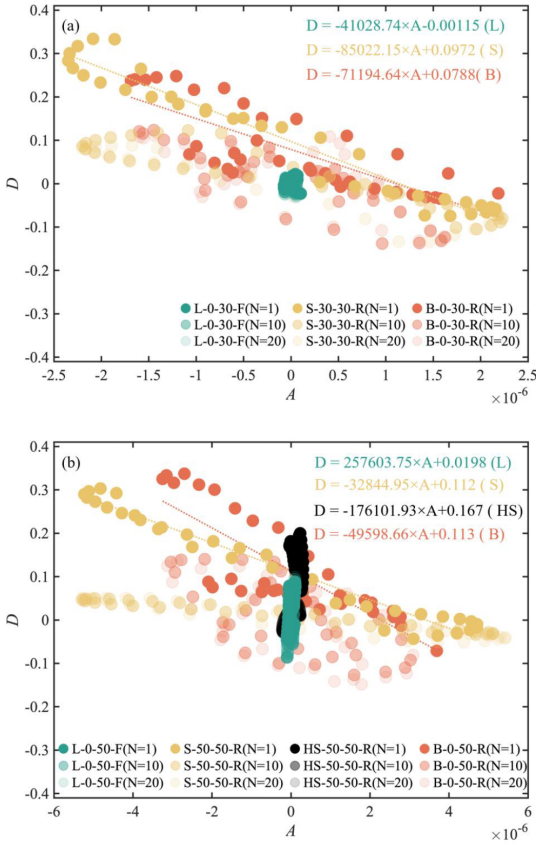

Figure 9: Scatter plot of dilatancy versus A at 1st, 10th, 20th cycle for tests of stress value and orientation change within a fixed plane: (a) series 1; (b) series 2 and series 3. The linear fit between dilatancy D and the initial fabric anisotropy variable A for the first load cycle is also plotted for reference.

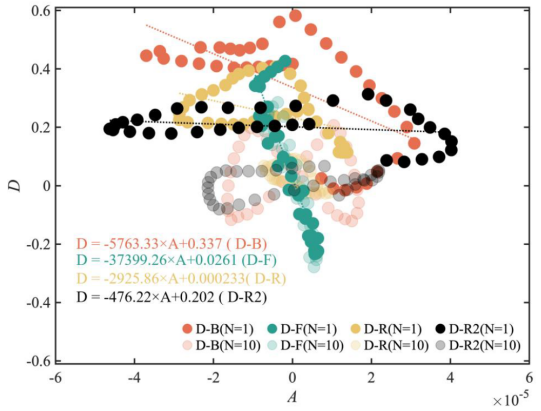

Figure 13: Load-displacement curves obtained in the three-point bending test presented in Subsection 2.6 for the same two mesh sizes as those presented in the manuscript, but with a phenomenological damage model that exhibits full softening.

Reply to Reviewer 2

We are very grateful to the reviewer for the encouraging comments. We have carefully revised the manuscript and listed the responses of the comments by the reviewer as follows. We believe the quality of our manuscript has been improved with this revision.

- Page 2: For the readers it would be helpful to add a notation overview (e.g. equivalent shear strain, dilatancy D, fabric anisotropy value A, ...).

As recommended by the reviewer, a list of symbols is added in the article in front of the 'Introduction' section in Page 2.

List of Symbols

D_{50}	The portions of particles with diameters smaller and larger than this value are 50%
$D_{\min}$	Minimum particle diameter within the sample
$D_{\max}$	Maximum particle diameter within the sample
r	Radius of the sample
σ_{ij}	Stress tensor
s_{ij}	Deviatoric stress tensor
$\sigma_{1,2,3}$	Deviatoric stress tensor
p	Mean effective stress
τ_{ij}	Shear stress at i direction, perpendicular to j direction
q	Deviatoric stress
$q_{\min}$	Minimum deviatoric stress during simulation
$q_{\max}$	Maximum deviatoric stress during simulation
ε_{ij}	Strain tensor
e_{ij}	Deviatoric strain tensor
ε_v	Volumetric strain
γ	Equivalent shear strain
F_{ij}	Deviatoric contact fabric tensor
G	Shear modulus
δ_{ij}	Kronecker delta
G	Shear modulus
I_m	Friction mobilization index
D	Dilatancy

- Page 2, right column, fourth paragraph: I recommend to explain Δl in more detail.

Δl is the interval length of force lines distribution. To be clear, Δl is plotted in Fig. (1). In Page 3:

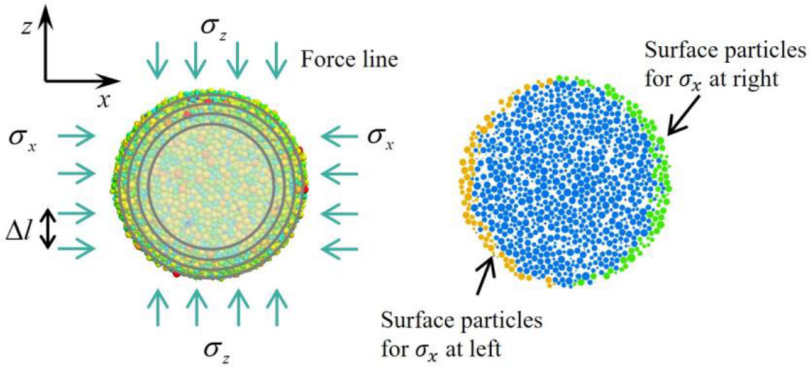

Figure 1: Schematic diagram of the sphere sample (21540 particles, e=0.686 ~ 0.689) and force line method for the application of stress. Note that the actual applied force line is much more densely distributed.

- Page 3, right column, fourth paragraph: why are definitions of an "Average" only in the equations (4),(5) and (6) used, but not in the other equations from (1)-(9)?

  All the quantities calculated in the article are particle-based or contact-based, which is the average over the whole sample. Equation (4), (5) and (6) define the calculation of average strain, while equation (1) is the stress and equation (9) is the fabric tensor, both of which are averages over the whole sample as well. The other quantities such as mean stress, shear stress, and equivalent shear strain is calculated based on the averaged quantities.

- Figure 1: Please include the range of the void ratio as well as the number of particles in the caption.

  As recommended by the reviewer, the range of the void ratio as well as the number of particles is included in the caption of Figure 1. In Page 3:

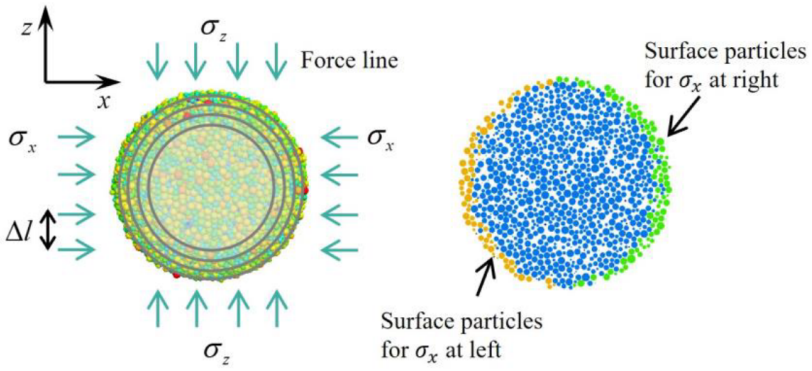

Figure 1: Schematic diagram of the sphere sample (21540 particles, e=0.686 ~ 0.689) and force line method for the application of stress. Note that the actual applied force line is much more densely distributed.

- Figure 2:
  - Page 3, the definition of mean effective stress p and deviatoric stress q is given in Eq. (2) and (3). Table 1 use these definitions for q_{min} and q_max. The left column of Fig. 2 is similar to Towhata and Ishihara [1], but using p and q as well as a definition of the Amplitude q_ampl the reader could follow more easily.
  - What are the units of x, y and z in the right column (cf. Fig. 10 in (kPa))?

  The definitions are added to the article. q_{min} and q_{max} are the minimum and the maximum deviatoric stress during test, respectively. We use them instead of q_{ampl} because the term amplitude can be somewhat ambiguous under the condition of pure stress orientation change, where the deviatoric stress does not change. The units of x, y and z in the right column is kPa, added to the figure.
  In Page 4:
  7 tests are conducted, as shown in Table (1), where q_{min} and q_{max} are the minimum and the maximum deviatoric stress during test, respectively.
  In Page 5:

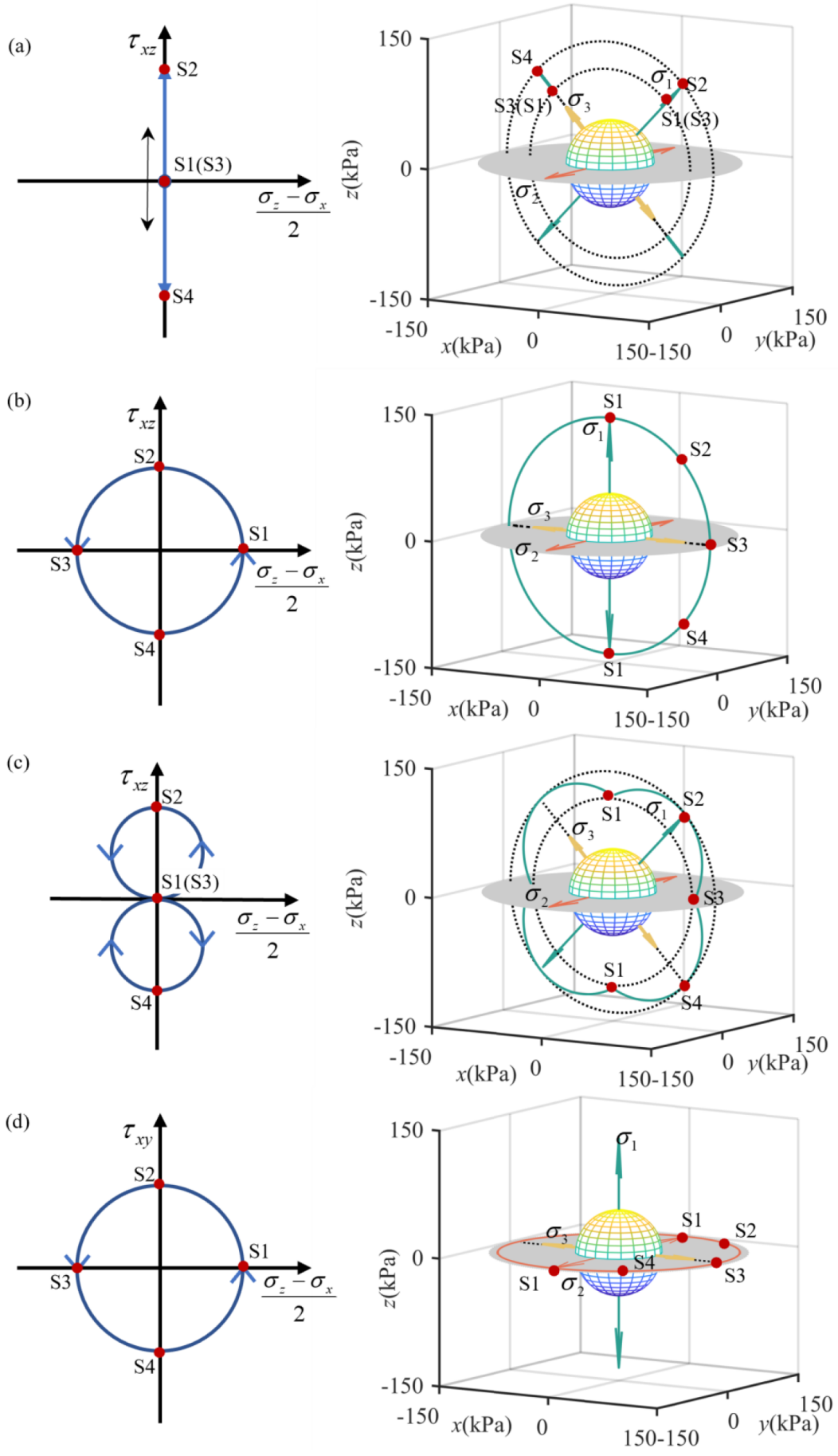

Figure 2: Stress paths for tests of stress value and orientation change within a fixed plane: (a) Straight-line; (b) Circular; (c) "8"-shaped; (d) Circular (Horizontal).

- Page 5, left column: Please refer the Figures 2b-d in the text.

  Figures 2b-d is referred to in section 3.1, as suggested by the reviewer.

- Page 5, left column, first paragraph of 3.2: Eventually, the accumulation of volumetric strain slows down to reach an asymptotic state, as discussed by Wang et al. [2019b] and Xue et al. [2019]. Eventually? This aspect should not be questioned by the authors.

  The expression has been changed in the article.
  In Page 4:
  Such accumulation would slow down, and the volumetric strain would reach an asymptotic state [Wang et al., 2019b; Xue et al., 2019].

- Figure 3:
  (1) The figures 3(a) and 3(b) should be scaled identically.
  (2) It's interesting to see that the test results in Fig. 3(a) for L-0-30-F with qmax = 30 kPa $\rightarrow \varepsilon_v(\mathrm{N}=30) \approx 1 \cdot 10^{-4}$ are comparable to the results of Wichtmann and Knittel Wichtmann and Knittel [2019] in Fig. 17.
  (3) In Fig. 3(a) for S-30-30-R with $q_{max} = q_{min} = 30$ kPa $\rightarrow \varepsilon_v(\mathrm{N}=30) \approx 2.1 \cdot 10^{-3}$ is received. The comparison with L-0-30-F results in a factor of 20 in volumetric strain. On the physically side, this seems to be impossible. Could the authors explain these distinguish results?
  (4) From Fig. 3(b) for L-0-50-F $\rightarrow \varepsilon_v(\mathrm{N}=30) \approx 1 \cdot 10^{-3}$ and S-50-50-F $\rightarrow \varepsilon_v(\mathrm{N}=30) \approx 8.5 \cdot 10^{-3}$ a factor of 8.5 in volumetric strain can be estimated. Why does a higher amplitude take more than two times lower in volumetric strain by comparison of 3(a) and 3(b)?
  (5) Comparison of HS-50-50-R and S-50-50-R: could the authors describe this discrepancy even though the planes are just rotated?

  (1) The figures 3(a) and 3(b) have been scaled identically.
  (2) A comparison with the results of Wichtmann and Knittel is added.
  (3) For L-0-30-F and S-30-30-R, owing to small shear stress ratio, there is very little plastic volumetric strain accumulation for L-0-30-F. Whereas more plastic deformation is induced under principal stress orientation change, resulting in the significant difference between L-0-30-F and S-30-30-R.
  (4) When the shear stress ratio increases, the plastic strain of the sample significantly increases for the fixed stress orientation loading case, and a smaller difference between L-0-50-F and S-50-50-R is observed. It shows that the stress amplitude is also an important influence factor.
  (5) For HS-50-50-R and S-50-50-R, as mentioned before, natural deposit process is used to generate the sample, resulting in initial anisotropy. The sample is more easily to be compressed when the major principal stress is rotated to horizontal plane, which is achieved in S-50-50-R. When the major principal stress is in the vertical direction, the sample is more difficult to be compressed, in HS-50-50-R. Therefore, the volumetric strain under S-50-50-R is much greater than that of HS-50-50-R.

- Page 5, right column, first paragraph: These results agree qualitatively with the undrained cyclic torsional tests by Towhata and Ishihara Towhata and Ishihara [1985], which showed that the liquefaction resistance of sand under a half-"8"-shaped stress path is between circular stress path and straight-line stress path. This statement is correct, however, it would be easier for the reader to depict an figure in the text with this statement.

  Towhata and Ishihara compared the liquefaction resistance of half-"8"-shaped stress path and straight-line stress path in the figure. The findings are only qualitatively comparable to the current study and may not provide a direct quantitative comparison. Therefore, we have chosen not to add the figure from their work to the current manuscript.

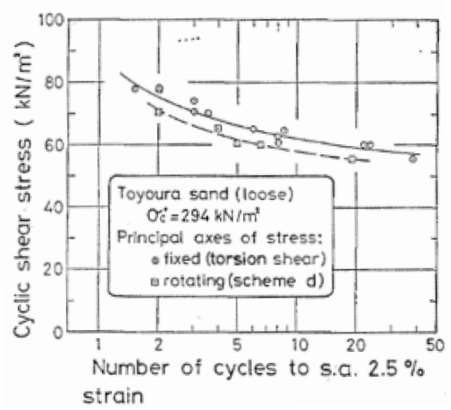

Liquefaction curves obtained by pore water pressure measurement [Towhata and Ishihara, 1985].

References:
Towhata, I. and Ishihara, K. (1985). Undrained strength of sand undergoing cyclic rotation of principal stress axes. Soils and Foundations, 25(2):135–147.

- Figure 4:
  (1) The figures 4(a) and 4(b) should be scaled identically.
  (2) Analogous to Fig. 3 the results of the equivalent shear strain are not consistent. Could the authors explain the comparison of the test results from S-30-30-R $\bar{\gamma}(N = 30) \approx 0.3$ and S-50-50-R $\bar{\gamma}(N = 30) \approx 1.3$ as an example?

  (1) As suggested by the reviewer, the figures 4(a) and 4(b) have been scaled identically.
  (2) For S-30-30-R and S-50-50-R, similar to volumetric strain, plastic sliding is triggered with greater deviatoric stress amplitude, resulting in larger plastic deformation accumulation.

- Figure 5:
  (1) The presented progress of the shear modulus G seems to be really small. Could the authors explain this physically in the text?
  (2) What is the cause of the spikes in G for L-0-30-F (numerical problems)?
  (3) S-30-30-R should be more critical as L-0-30-F, but no spikes occurred. The question is why?

  (1) We have checked the modulus again and found that the label used the wrong unit. It should be MPa. We have corrected this in the article.
  (2) For L-0-30-F, the strain interval between each step is very small, which could cause large numerical calculation error in G. To improve the calculation, a constant shear strain interval is now chosen to calculate the shear modulus shown in the article.
  (3) The strain per step is larger in the S-30-30-R case, resulting in fewer spikes. The current revision unifies the results.

  In Page 7: In Page 13:

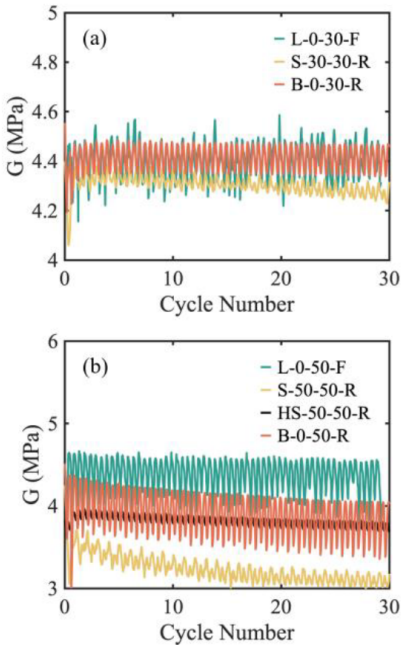

Figure 5: Shear modulus for tests of stress value and orientation change within a fixed plane: (a) series 1; (b) series 2 and 3.

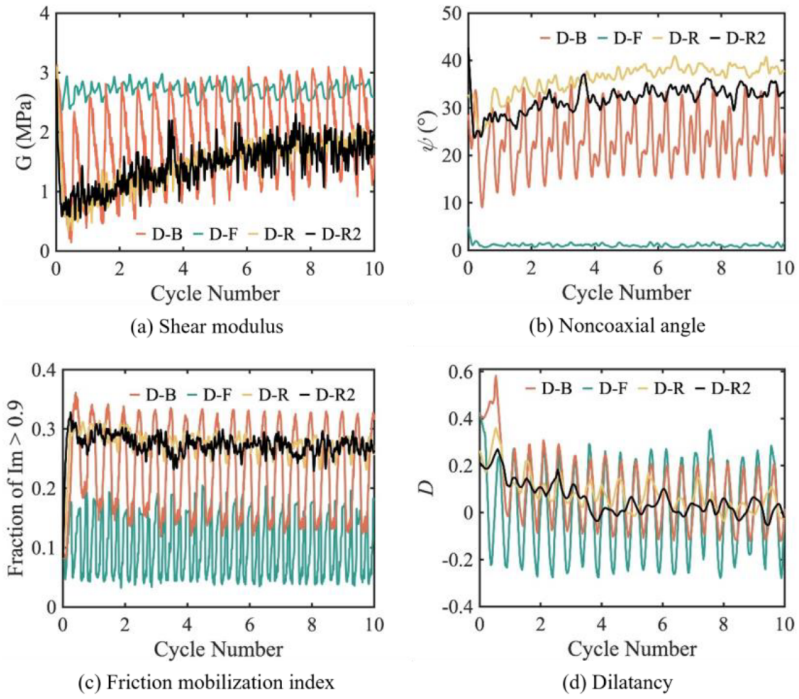

Figure 12: Shear modulus, non-coaxial angle, friction mobilization index and dilatancy of the seismic load simulation stress paths tests D-B, D-F, D-R, and D-R2.

- Figure 6: Please explain the differences in the amplitudes of B-0-30-R and S-30-30-R.

Similar to strain, shear stress ratio and principal stress rotation are important factors influencing the response of the sample. In S-30-30-R, the deviatoric stress is constant at q = 30 kPa while the orientation of the principal stress changes, and non-coaxial angle shows small oscillations around 42^o, and reaches its peak when major principal stress is rotated to the horizontal plane. However, In B-0-30-R, the deviatoric stress value changes as the principal stress orientation changes. When the major principal stress is rotated to the horizontal plane, the deviatoric stress is 0 kPa, resulting in a small non-coaxial angle.

In Page 7:
In S-30-30-R, the deviatoric stress is constant at q = 30 kPa while the orientation of the principal stress changes, and non-coaxial angle shows small oscillations around 42^o, and reaches its peak when major principal stress is rotated to the horizontal plane. However, In B-0-30-R, the deviatoric stress value changes as the principal stress orientation changes, resulting in violent fluctuation of non-coaxial angle. When the major principal stress is rotated to the horizontal plane, the deviatoric stress is 0 kPa, resulting in a small non-coaxial angle.

- Figure 9:
- This figure shows the dilatancy D and fabric anisotropy variable A, also at the 20th cycle with greater fluctuations. Fig. 3-7 is plotted for $0 \leq N \leq 30$ but Fig. 8 for $0 \leq N \leq 10$. Did the authors receive impossible values of D for $10 \leq N \leq 30$ in Fig. 8, which could be seen in Fig. 9?

As mentioned in the article, after few cycles, the volumetric strain of the sample becomes stable and the dilatancy fluctuates around zero for all simulations. Therefore, to show the dilatancy more clearly especially during each cycle, only first 10 cycles' dilatancy is plotted. As recommended by the reviewer, the dilatancy of all 30 cycles is plotted along with a closeup view of the first few cycles. In Page 9:

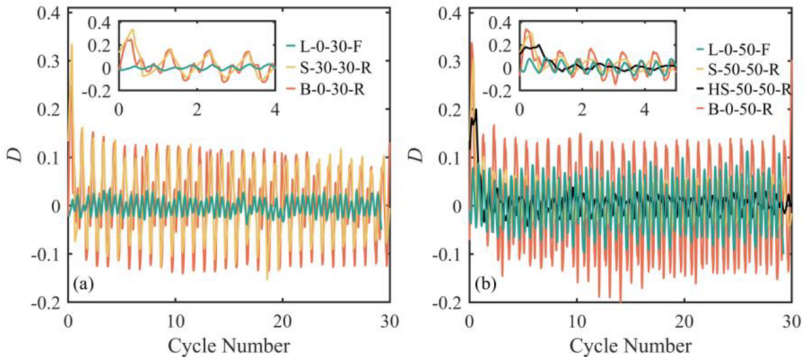

Figure 8: Shear modulus, non-coaxial angle, friction mobilization index and dilatancy of the seismic load simulation stress paths tests D-B, D-F, D-R, and D-R2.

- Figure 10: Please plot N = 30 cycles in Figure 10(b).

As recommended by the reviewer, N = 30 cycles are plotted.
In Page 11:

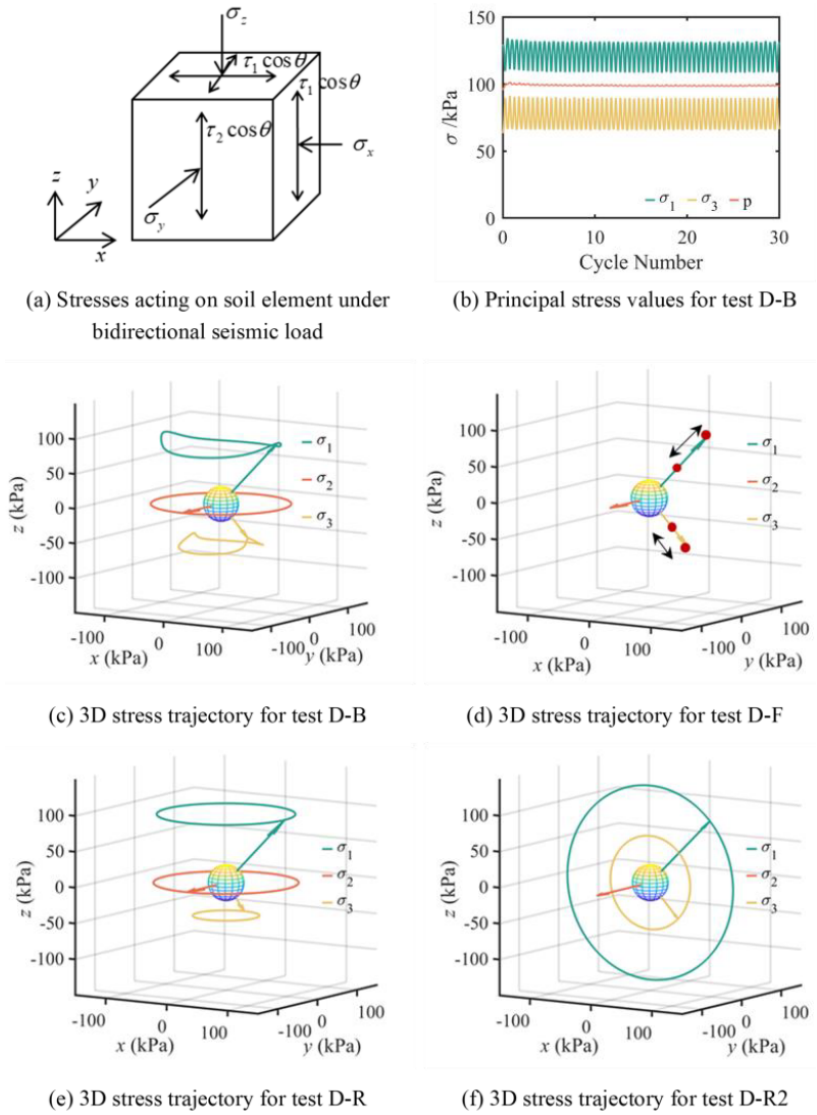

(a) Stresses acting on soil element under bidirectional seismic load

(b) Principal stress values for test D-B

(c) 3D stress trajectory for test D-B

(d) 3D stress trajectory for test D-F

(e) 3D stress trajectory for test D-R

(f) 3D stress trajectory for test D-R2

Figure 10: Stress paths for bidirectional seismic stress path tests, including bidirectional seismic stress path test D-B, pure principal stress value change test D-F, pure 3D principal stress orientation change test D-R, and pure principal stress orientation with respect to σ_2 test D-R2.

- What is the practical relevance for N = 30 number of seismic load cycles? What is the physical time for seismic loads (of course no time dependence were considered)?

  N=30 is the number of cycles that would be large enough to let the sample accumulate significant strain or even get to a stable strain accumulation. All the tests conducted here are quasistatic and there is no time dependency.

- Page 13, last paragraph of the conclusion: ... all possible influence factors, which warrants more in-depth investigations. Which ones? Please give some hints.

  As recommended by the reviewer, some possible factors are listed in the end of the article.
  In Page 13:
  The observations made in this study are from a limited set of DEM numerical tests and do not exhaustively assess all possible influence factors, like mean stress, void ratio, and particle shape, which warrant more in-depth investigations.

Review Round 2

Reviewer 1 (Konstantinos Karapiperis)

The authors have properly addressed the points that were raised. I recommend the paper for publication.

Reviewer 2 (Lukas Knittel)

Recommendation: Accept Submission, no comments.

Editor decision

At the end of Review Round Number 2, the managing Editor has decided to accept the revised version of the manuscript for publication without any further changes.

References

L. Xue, N.P. Kruyt, R. W. and Zhang, J.-M. (2019). 3D dem simulation of principal stress rotation in different planes of cross-anisotropic granular materials. *International Journal of Numerical and Analytical Methods in Geotechnics*, 43:2227–2250.

Towhata, I. and Ishihara, K. (1985). Undrained strength of sand undergoing cyclic rotation of principal stress axes. *Soils and Foundations,*, 25:135–147.

Wichtmann, T. and Knittel, L. (2019). Behaviour of granular soils under uni- and multidimensional drained high-cyclic loading. In Triantafyllidis, T., editor, *Recent Developments of Soil Mechanics and Geotechnics*, Theory and Practice, pages 136–165. Springer.